Journal of Statistical Physics, Vol. 67, Nos. 3/4, 1992

Properties of a Three-Dimensional Poisson–Voronoi Tesselation: A Monte Carlo Study

Susmit Kumar,[1] Stewart K. Kurtz,[1,2] Jayanth R. Banavar,[1,3] and M. G. Sharma[4]

Received October 8, 1991; final January 2, 1992

A complete statistical description of the properties of a cellular microstructure generated by a three-dimensional Poisson–Voronoi tesselation has been obtained by a rigorous computer simulation involving several hundred thousand cells. A two-parameter gamma distribution is found to be a good fit to the cell's face, volume, and surface area distributions. For a sample size of several thousand cells or less, a lognormal distribution can also be used to approximate these distributions. The individual face, area, and edge length distributions are also obtained.

KEY WORDS: Voronoi cell; Poisson; gamma distribution; lognormal distribution.

1. INTRODUCTION

The Voronoi tesselation is a convenient and powerful method to carry out a random subdivision of space. It has been widely used as a model in the study of the liquid structure,[1] polycrystalline structure,[2] protein structure,[3] fragmentation of the universe,[4,5] in metallurgy,[6] biology,[7] and geography.[8]

According to the definition of a Voronoi tesselation, a Voronoi cell

[1] Materials Research Laboratory, Pennsylvania State University, University Park, Pennsylvania 16802.

[2] Department of Electrical and Computer Engineering, Pennsylvania State University, University Park, Pennsylvania 16802.

[3] Department of Physics, Pennsylvania State University, University Park, Pennsylvania 16802.

[4] Department of Engineering Science and Mechanics, Pennsylvania State University, University Park, Pennsylvania 16802.

0022-4715/92/0500-0523$06.50/0

associated with a nucleus P in space contains all points in that space which are closer to P than to any other nucleus. The Voronoi tesselation thus produces convex polyhedral cells which have planar faces and completely fill the space. Most important from a physical point of view, the topology of the resulting cellular network is similar to that of ceramic and metallurgical microstructures. That is, every edge connects three gains and two vertices, and every vertex connects four edges, six faces, and four grains. Thus, a topological similarity exists, which is readily seen in Fig. 1.

As emphasized in the seminal work of Smith[9] and expanded on by others (e.g., Rhines and Craig[10]), the topology of each grain in such a microstructure is characterized by a single parameter, which we take to be its number of faces F. One can then distinguish topological classes of grains which in metals and ceramics vary from $F = 4$ to 36, i.e., ~ 33 classes

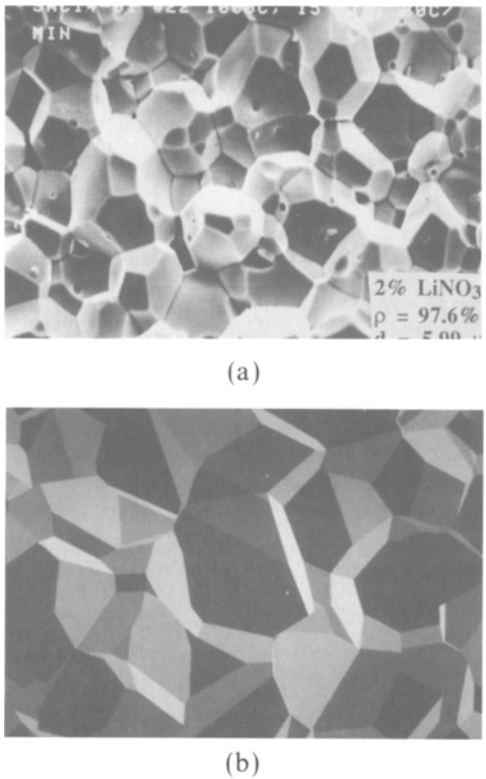

(a)

(b)

Fig. 1. (a) Three-dimensional microstructure revealed in the intragranular fracture cross section of polycrystalline electroceramic $PbMg_{1/3}Nb_{2/3}O_3$ (lead magnesium niobate). (b) Topologically similar three-dimensional Poisson–Voronoi microstructure from the present work.

with mean $\bar{F} \sim 14$–15 and volume increasing monotonically with increasing topological class.

A statistical model of grain growth based on an assumed lognormal distribution of grains by topological class and by size was developed by one of the authors.[11] This model has received some attention,[12] but has been criticized because of a lack of theoretical basis for the lognormality assumed in its formulation. The present work was motivated in part by the desire to investigate in somewhat greater detail the statistical topology of a topologically equivalent microstructure for a case where complete access to three-dimensional properties of a very large numbers of grains would be possible.

Similar detailed analyses of the two-dimensional statistical topology of a Poisson–Voronoi tesselation have been carried out by Hinde and Miles[13] and Gilbert.[14] The present work is built in large part on their groundbreaking efforts and is intended to provide a comprehensive statistical characterization of the three-dimensional Poisson–Voronoi tesselation. In later papers we will describe real-time graphical display of microstructures containing 1000–10,000 grains and development of a finite element analysis package which we have successfully used to calculate the elastic moduli of simulated metal and ceramic microstructures.

Meijering[15] in his classic paper studied the topological properties of the Voronoi cells, giving theoretical results for the mean value of the number of faces, edges, and vertices. Gilbert[14] analytically calculated the variances of their statistical distributions. To date, no exact closed-form solution has been found for these discrete statistical distributions.

In the past decade, numerous researchers[16–19] have studied the characteristics of the Voronoi cells using computer simulation. In general their simulations were for a few thousand cells, which we show in this study is inadequate to distinguish subtle differences in the statistics. In order to obtain accurate results for the statistical distributions of topological and size parameters, we have used a Monte Carlo method to simulate several hundred thousand Voronoi cells in three dimensions.

It will be shown that the face, volume, and surface area distributions of the Poisson–Voronoi cells are best described by the gamma distribution with appropriate choice of parameters. The gamma distribution with two parameters a and b is described by

$$P_{x,x+dx} = \frac{x^{a-1}}{b^a \Gamma(a)} e^{-x/b}\, dx, \qquad x > 0$$

where the mean and the variance of the distribution are ab and ab^2, respectively.

Our study also shows that for sample sizes less than about 5000 cells, the face, volume, and surface area distributions of the Voronoi cells can be approximated by a lognormal distribution.[5] This is due to the fact that for the ranges of the parameters for these distributions found in the Poisson–Voronoi tesselation, there is a negligible difference between the two distributions.[20]

2. ALGORITHM

In the Voronoi tesselation of space, the topological conditions to be satisfied for each individual polyhedron are (i) $V+F-E=2$ and (ii) $V=2F-4$, where V is the number of vertices, F is the number of faces, and E is the number of edges.

We have used these conditions to write an efficient algorithm to generate a Voronoi structure in three dimensions. The steps of the algorithm are:

(i) Define a region R containing N nuclei to generate N Voronoi cells.

(ii) Calculate the maximum distance between the ith nucleus and any of the points in the region R, denoted by $d_{\max}[i]$, $i=1, 2,..., N$.

(iii) Calculate the minimum distance between the ith nucleus and any of the points in the region R, denoted by $d_{\min}[i]$, $i=1, 2,..., N$.

(iv) Calculate the minimum of $d_{\max}[i]$, $i=1, 2,..., N$, say

$$m=\min\{d_{\max}[i]\}$$

(v) Find those nuclei for which $d_{\min}[i]\leqslant m$. Let this condition be satisfied by $N1$ nuclei $(i_1, i_2,..., i_{N1})$.

(vi) (a) If $N1\leqslant 3$, stop.

(b) However, if $N1=4$, and the volume of region R is less than ε (a predetermined small number which depends on the nuclear density; in the Monte Carlo portion of the study, for $N=300$ nuclei in a unit cube, $\varepsilon=1.0\times 10^{-22}$), then the coordinates of the vertex common to i_1, i_2, i_3, and i_4 are those of the center of the sphere which passes through the i_1, i_2, i_3, and i_4 nuclei.

(c) If $\{(N1>4)\}$ or $\{(N1=4)$ and (volume of region $R>\varepsilon)\}$,

[5] The lognormal distribution with two parameters $\sigma_{\ln}$ and x_{50} is described as

$$P_{x,x+dx}=\frac{1}{\sigma_{\ln}(2\pi)^{1/2}}\exp\left[-\frac{(\log_e x-\log_e x_{50})^2}{2\sigma_{\ln}^2}\right]dx, \qquad x>0$$

Table I. Normalization Constants[a]

Variable	Normalization constant
Volume	ρ^{-1}
Surface area	$\rho^{-2/3}$
Face area	$\rho^{-2/3}$
Edge length	$\rho^{-1/3}$

[a] In the present paper the density of nuclei $\rho = 300$ nuclei in a unit cube.

divide the region R into two or more subregions and repeat from step (ii), taking $(i_1, i_2, ..., i_{N1})$ nuclei into account.

After finding all the vertices in the system, one can easily find the numbers of faces and edges for a specific Voronoi cell by searching its vertices and finding the identities of the corresponding nuclei with which it shares the vertices. One test regarding the smallness of ε is to verify that all the polyhedra satisfy the topological constraints (i) $V+F-E=2$ and (ii) $V=2F-4$. This algorithm is very efficient compared to that of Mahin *et al.*[19] because it searches only the vertices and not the edges and the faces, which take much more time. The computation time is thus drastically reduced.

For the Monte Carlo calculation of the properties of the Voronoi cells, we generated 300 (Poisson-distributed) random nuclei within a unit cube, with one of the points at the center of the cube. We then calculated the properties of the Voronoi cell associated with the central nucleus. This Voronoi cell was not included in the analysis if one (or more) of its corners was on the face of the cube. This typically occurred about ten times in the process of generating 358,000 cells. We have accumulated statistics,

Table II. Properties of Voronoi Cells

	Faces	Volume	Surface area	Edge length per cell	Edge per face
Expected (mean)	15.5355	1.0000	5.8209	17.4956	5.2260[a]
Calculated (mean)	15.5431	1.0011	5.8267	17.5204	5.2280
Maximum	36.0000	4.0870	13.8315	—	15.0000
Minimum	4.0000	—	—	—	3.0000
Standard deviation	3.3350	0.4198[b]	1.4635	—	1.5763
Skewness	0.1738	0.3937	0.1549	—	0.4307
Kurtosis (−3)	0.0998	0.8108	0.0464	—	0.1431

[a] Santalo.[23]

[b] Expected value is 0.424.[14]

indicating a negligible but nevertheless nonzero bias. As Hanson[17] had earlier found faces out to the 98th nearest neighbor, we chose 300 Poisson points within the cube, so that there would be

$$\frac{4\pi}{3} \times \left(\frac{1}{2}\right)^3 \times 300 \cong 157$$

Poisson points within the sphere embedded within the cube, i.e., 156 neighboring cells for the central cell in the cube.

Table III. Face Distribution (Based on 358,000 Simulated Cells)

Faces	Frequency	Probability	Hanson[17]
4	2	5.5866e−6	0
5	10	2.7933e−5	3.3333e−4
6	117	3.2682e−4	3.3333e−4
7	570	1.5922e−3	2.0000e−3
8	2080	5.8101e−3	3.3333e−3
9	5347	1.4936e−2	1.5000e−2
10	11057	3.0885e−2	2.6667e−2
11	18657	5.2115e−2	5.1333e−2
12	27548	7.6950e−2	7.7000e−2
13	35947	1.0041e−1	9.3000e−2
14	41044	1.1465e−1	1.0633e−1
15	42699	1.1927e−1	1.2800e−1
16	41117	1.1485e−1	1.2667e−1
17	36316	1.0144e−1	9.7667e−2
18	29515	8.2444e−2	8.5333e−2
19	22643	6.3249e−2	6.6000e−2
20	16193	4.5232e−2	4.6000e−2
21	10962	3.0620e−2	2.8333e−2
22	6927	1.9349e−2	2.0000e−2
23	4167	1.1640e−2	1.1000e−2
24	2406	6.7207e−3	6.3333e−3
25	1366	3.8156e−3	5.3333e−3
26	665	1.8575e−3	1.0000e−3
27	349	9.7486e−4	1.3333e−3
28	179	5.0000e−4	1.3333e−3
29	71	1.9832e−4	0
30	22	6.1453e−5	3.3333e−4
31	14	3.9106e−5	0
32	5	1.3966e−5	0
33	1	2.7933e−6	0
34	2	5.5866e−6	0
35	1	2.7933e−6	0
36	1	2.7933e−6	0

3. RESULTS

Table II shows a list of the important parameters for Voronoi cells along with those deduced analytically by previous workers. Tables III–V and Figs. 2–4 show the various statistical distributions of the faces and the edges of the Voronoi cells. These results are based on the simulation of 358,000 Voronoi cells.

Tables VI and VII and Figs. 5–10 show the distributions of volume and surface area of the Voronoi cells. Data points were grouped into intervals defined in the figure captions. Tables VIII and IX and Figs. 11–14 show the statistical properties of the area of the individual faces. Tables VIII and IX and Figs. 15–17 show the properties of the lengths of the individual edges of the Voronoi cells. Figure 18 is a plot of the mean total edge length of the Voronoi cell having a fixed number of faces, which was calculated by multiplying the mean length of an edge by the number of edges corresponding to the number of faces, i.e., $(3 \times \text{number of edges} - 6)$. Figure 19 shows the plot of the mean perimeter for faces having a fixed number of edges. These data are based on the simulation of 102,000 Voronoi cells.

Figure 20 shows the probability distribution (based on the simulation of 148,000 Voronoi cells) of the use of nearest neighbors of a point in forming a Voronoi cell face. Figure 21 shows a plot of the mean number of faces $\bar{F}_F$ of neighboring cells for the subset of cells having a fixed number of faces, designated by the integer subscript F.

Table IV. Distribution of n-Sided Faces (Based on 358,000 Simulated Cells)

Sides	Frequency	Probability	Hanson[17]
3	748304	1.3448e − 1	1.3545e − 1
4	1280529	2.3013e − 1	2.2904e − 1
5	1344428	2.4161e − 1	2.4121e − 1
6	1058408	1.9021e − 1	1.8963e − 1
7	648015	1.1646e − 1	1.1511e − 1
8	313743	5.6384e − 2	5.8385e − 2
9	120637	2.1680e − 2	2.1963e − 2
10	37951	6.8203e − 3	6.6743e − 3
11	9843	1.7689e − 3	1.8125e − 3
12	2121	3.8117e − 4	6.3971e − 4
13	381	6.8471e − 5	6.3971e − 5
14	56	1.0064e − 5	2.1324e − 5
15	14	2.5160e − 6	0

Table V. Edge Distribution for *n*-Faced Cells (Based on 358,000 Simulated Cells)

Number of faces	Mean number of edges	Standard deviation	Skewness	Kurtosis (−3)
4	3.0000			
5	3.6000	0.4899	−0.2041	−1.8333
6	4.0000	0.7000	0.0000	−0.9593
7	4.2857	0.8546	0.1336	−0.6691
8	4.5000	1.0071	0.2208	−0.5759
9	4.6667	1.1239	0.2724	−0.4618
10	4.8000	1.2232	0.3140	−0.3846
11	4.9091	1.3081	0.3458	−0.3400
12	5.0000	1.3769	0.3724	−0.2723
13	5.0769	1.4410	0.3953	−0.2067
14	5.1429	1.4909	0.4088	−0.1539
15	5.2000	1.5376	0.4268	−0.0940
16	5.2500	1.5763	0.4321	−0.0540
17	5.2941	1.6142	0.4480	−0.0169
18	5.3333	1.6454	0.4488	0.0516
19	5.3684	1.6740	0.4602	0.0804
20	5.4000	1.7024	0.4648	0.1247
21	5.4286	1.7228	0.4699	0.1289
22	5.4545	1.7413	0.4716	0.1885
23	5.4783	1.7633	0.4820	0.1620
24	5.5000	1.7755	0.4815	0.1830
25	5.5200	1.7944	0.4901	0.1813
26	5.5385	1.7981	0.4844	0.2024
27	5.5556	1.8148	0.4811	0.2845
28	5.5714	1.8115	0.4751	0.0782
29	5.5862	1.8608	0.5026	0.1450
30	5.6000	1.8391	0.4923	0.6832
31	5.6129	1.8928	0.4835	0.5977
32	5.6250	2.1118	0.9848	1.0677
33	5.6364	1.7721	0.9279	−0.9723
34	5.6471	1.6783	0.2385	0.4081
35	5.6571	1.7062	1.6851	−0.1933
36	5.6667	2.0548	3.3730	0.1579

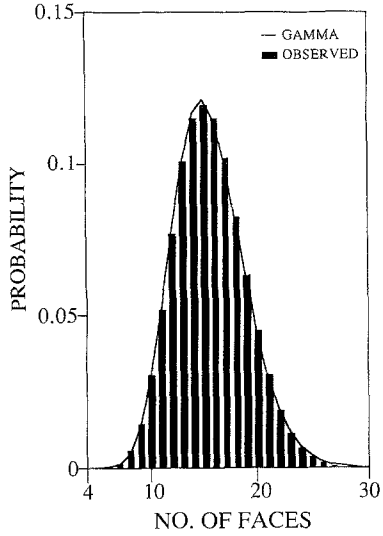

Fig. 2. The probability distribution of faces for 3D Poisson–Voronoi tesselations. This is based on 358,000 simulated cell data (histogram). The best-fit (discretized) gamma distribution with parameters $a = 21.6292$ and $b = 0.7199$ is shown by continuous line.

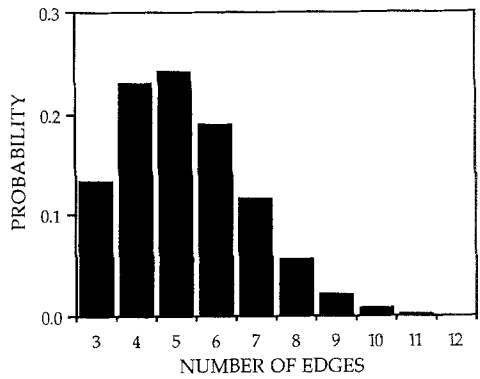

Fig. 3. The probability distribution of edges for the 3D Poisson–Voronoi tesselation obtained on the basis of 358,000 simulated cells.

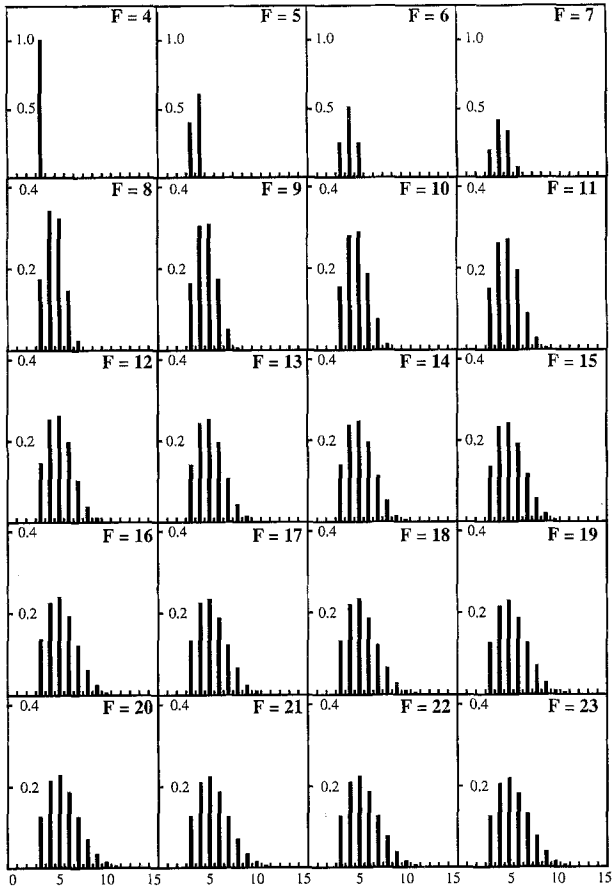

Fig. 4. The probability distribution of edges for the Voronoi cells having a fixed number of faces F obtained on the basis of 358,000 simulated cells. The vertical axis and the horizontal axis denote the probability and the number of edges, respectively. (a) 4–23 faces, (b) 24–27 faces.

Table VI. Volume Distribution (Based on 102,000 Simulated Cells)[a]

Face	Number of simulated cells	Observed mean	Observed variance	a	b	Max $\lvert f_{obs} - f_{fit} \rvert$	KS limit 1% $1.52/\sqrt{n}$	KS limit 5% $1.22/\sqrt{n}$
6	26	0.2159	0.0132	3.7575	0.0567	0.0169	0.2900	0.2350
7	152	0.2881	0.0161	5.2135	0.0552	0.0135	0.1233	0.0990
8	535	0.3497	0.0211	6.7192	0.0511	0.0297	0.0657	0.0527
9	1512	0.4307	0.0275	7.0034	0.0610	0.0119	0.0391	0.0314
10	3112	0.5069	0.0327	8.2030	0.0619	0.0031	0.0272	0.0219
11	5359	0.5859	0.0411	8.6072	0.0680	0.0030	0.0208	0.0167
12	7860	0.6694	0.0478	9.7169	0.0688	0.0024	0.0171	0.0138
13	10285	0.7599	0.0555	10.8460	0.0700	0.0027	0.0150	0.0120
14	11719	0.8518	0.0640	11.7293	0.0725	0.0040	0.0140	0.0113
15	12037	0.9418	0.0735	12.2455	0.0769	0.0028	0.0139	0.0111
16	11712	1.0336	0.0833	12.9683	0.0797	0.0027	0.0140	0.0113
17	10424	1.1286	0.0899	14.5232	0.0776	0.0028	0.0149	0.0119
18	8583	1.2246	0.1006	14.8625	0.0824	0.0026	0.0164	0.0132
19	6454	1.3161	0.1093	16.2205	0.0810	0.0054	0.0189	0.0152
20	4576	1.4261	0.1199	17.1804	0.0829	0.0029	0.0225	0.0180
21	3052	1.5160	0.1250	17.9044	0.0848	0.0056	0.0275	0.0221
22	1963	1.6221	0.1419	17.5351	0.0927	0.0090	0.0343	0.0275
23	1173	1.7289	0.1529	19.6118	0.0882	0.0085	0.0444	0.0356
24	677	1.8544	0.1662	19.7143	0.0940	0.0095	0.0584	0.0469
25	411	1.9578	0.1581	24.2285	0.0806	0.0092	0.0750	0.0602
26	200	2.0620	0.1772	23.4131	0.0883	0.0221	0.1075	0.0863
27	96	2.1541	0.1982	20.9337	0.1037	0.0322	0.1551	0.1245
28	50	2.2472	0.2208	23.6420	0.0961	0.0474	0.2150	0.1725

[a] f_{obs} is the observed cumulative probablity density; f_{fit} is the fitted cumulative probability density; KS, Kolmogrov–Smirnov.

Table VII. Surface Area Distribution (Based on 102,000 Simulated Cells)[a]

Face	Number of simulated cells	Observed mean	Observed variance	a	b	Max $\lvert f_{obs} - f_{fit} \rvert$	KS limit 1% $1.52/\sqrt{n}$	KS limit 5% $1.22/\sqrt{n}$
6	26	2.4258	0.3631	16.2053	0.1556	0.0755	0.2900	0.2350
7	152	2.8979	0.6522	12.3732	0.2351	0.0127	0.1233	0.0990
8	535	3.2430	0.6613	17.8586	0.1798	0.0309	0.0657	0.0527
9	1512	3.6625	0.7144	18.4058	0.1995	0.0068	0.0390	0.0314
10	3112	4.0094	0.7703	20.8798	0.1925	0.0081	0.0272	0.0219
11	5359	4.3364	0.8378	22.5648	0.1925	0.0063	0.0208	0.0167
12	7860	4.6830	0.8747	25.3588	0.1850	0.0039	0.0171	0.0138
13	10285	5.0334	0.9235	27.7469	0.1819	0.0054	0.0150	0.0120
14	11719	5.3707	0.9819	29.3245	0.1836	0.0050	0.0140	0.0113
15	12037	5.6887	1.0412	31.3959	0.1815	0.0051	0.0139	0.0111
16	11712	5.9941	1.0831	32.9717	0.1821	0.0037	0.0140	0.0113
17	10424	6.3158	1.0938	36.6227	0.1727	0.0060	0.0149	0.0119
18	8583	6.6149	1.1488	37.7694	0.1753	0.0042	0.0164	0.0132
19	6454	6.8992	1.1768	40.5935	0.1700	0.0047	0.0189	0.0152
20	4576	7.2304	1.2076	42.8758	0.1689	0.0048	0.0225	0.0180
21	3052	7.4970	1.1863	46.2693	0.1622	0.0083	0.0275	0.0221
22	1963	7.7899	1.2907	45.4076	0.1718	0.0057	0.0343	0.0275
23	1173	8.0917	1.3406	47.1423	0.1720	0.0114	0.0444	0.0356
24	677	8.4216	1.3893	52.9200	0.1592	0.0173	0.0584	0.0469
25	411	8.7243	1.1803	59.8812	0.1458	0.0209	0.0750	0.0602
26	200	8.9692	1.2849	64.7877	0.1382	0.0204	0.1075	0.0863
27	96	9.2428	1.3133	59.5848	0.1554	0.0240	0.1551	0.1245
28	50	9.5376	1.3000	55.2383	0.1727	0.0549	0.2150	0.1725

[a] f_{obs} is the observed cumulative probability density; f_{fit} is the fitted cumulative probability density; KS, Kolmogrov–Smirnov.

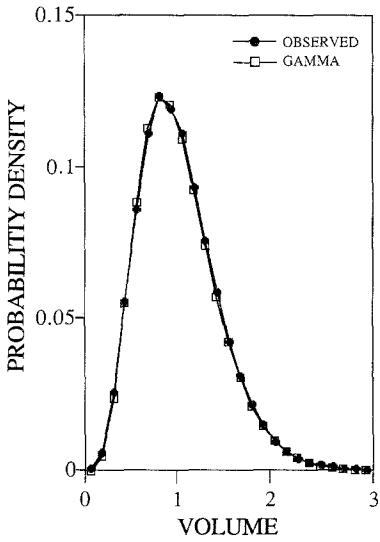

Fig. 5. The probability density distribution of cell volumes in 3D Poisson–Voronoi tesselation. This is based on 102,000 simulated cell data. The volume data were grouped in equal intervals of width 0.122. The best-fit gamma distribution with parameters $a = 5.6333$ and $b = 0.1782$ is also shown. See Table I and text for the description of the volume normalization factor.

Table VIII. Distributions of Area of Individual Faces and Length of Individual Edges for n-Edged Face (Based on 102,000 Simulated Cells)

Number of edges	Area of individual face		Length of individual edge	
	Mean	Standard deviation	Mean	Standard deviation
3	0.0457	0.0551	0.2509	0.2295
4	0.1385	0.1463	0.3823	0.2892
5	0.3043	0.2346	0.4481	0.3202
6	0.5047	0.2986	0.4725	0.3358
7	0.7092	0.3389	0.4730	0.3412
8	0.9067	0.3625	0.4623	0.3405
9	1.0918	0.3797	0.4466	0.3375
10	1.2632	0.3916	0.4289	0.3311
11	1.4331	0.3916	0.4130	0.3251
12	1.5606	0.4000	0.3927	0.3146
13	1.7656	0.4180	0.3842	0.3116
14	1.8388	0.3886	0.3642	0.2947
15	1.8594	0.3092	0.3345	0.2516

Table IX. Distribution of Length of Individual Edge and Area of Individual Face for *n*-Faced Cells (Based on 102,000 Simulated Cells)

Number of faces	Standard deviation of area distribution of individual face	Length of individual edge	
		Mean	Standard deviation
5	0.1735	0.6371	0.3734
6	0.2746	0.6710	0.3647
7	0.2930	0.5954	0.3383
8	0.3180	0.5539	0.3479
9	0.3316	0.5263	0.3454
10	0.3440	0.5031	0.3415
11	0.3516	0.4833	0.3373
12	0.3592	0.4687	0.3342
13	0.3667	0.4572	0.3311
14	0.3711	0.4460	0.3278
15	0.3758	0.4366	0.3259
16	0.3768	0.4281	0.3225
17	0.3804	0.4218	0.3207
18	0.3825	0.4152	0.3184
19	0.3834	0.4087	0.3162
20	0.3842	0.4045	0.3149
21	0.3852	0.3986	0.3125
22	0.3868	0.3950	0.3113
23	0.3878	0.3902	0.3097
24	0.3877	0.3887	0.3081
25	0.3854	0.3841	0.3062
26	0.3832	0.3815	0.3109
27	0.3772	0.3770	0.3003
28	0.3808	0.3773	0.3040
29	0.3714	0.3719	0.2960
30	0.3647	0.3698	0.3088
31	0.3642	0.3592	0.2871

The volume, surface area, area of individual face, and edge length of the cells are normalized by dividing them by constants. These normalization constants depend on the nuclear density within the chosen volume. They are given in Table I for each type of variable.

4. DISCUSSION

4.1. Face and Edge Distribution

The mean number of faces from our simulation, $\bar{F}$ is 15.5431, which is very near Meijering's exact result[15] ($\bar{F} = 48\pi^2/35 + 2 = 15.5355$) and

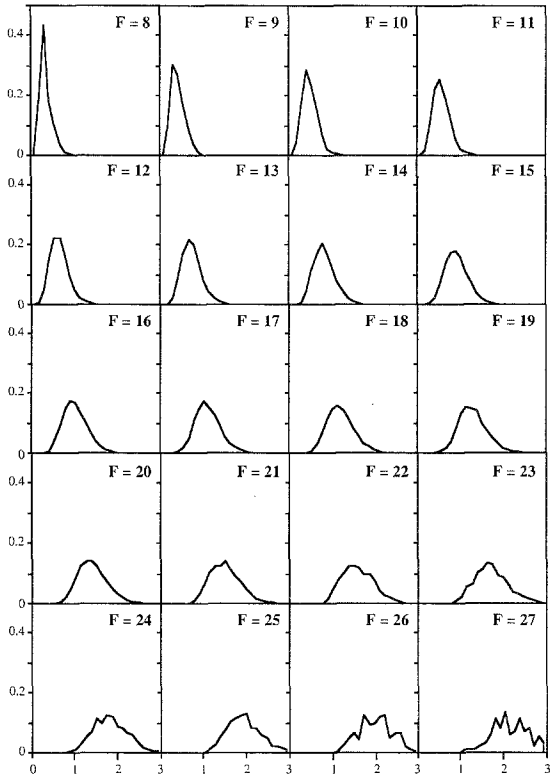

Fig. 6. The probability density distribution of volume of Voronoi cells having a fixed number of faces F. This is based on 102,000 simulated cell data. The volume data were grouped in equal intervals of width 0.122. The vertical axis and the horizontal axis denote the probability density and the volume, respectively. See Table I and text for the description of the volume normalization factor. All the curves can be described by the gamma distribution with suitable parameters (listed in Table VI).

substantially better than those of Hanson[17] ($\bar{F}=15.63$) and Quine and Watson[21] ($\bar{F}=15.5052$).

Hinde and Miles[13] suggested a discretized three-parameter gamma distribution for the side (edge) distribution in the two-dimensional Poisson–Voronoi tesselation. Using their data, we found that the best-fit discretized two-parameter gamma distribution[6] has $a=21.254$ and

[6] Discretized gamma distribution:

$$f(n)=\int_{n-1/2}^{n+1/2}\frac{x^{a-1}}{b^a\Gamma(a)}e^{-x/b}\,dx$$

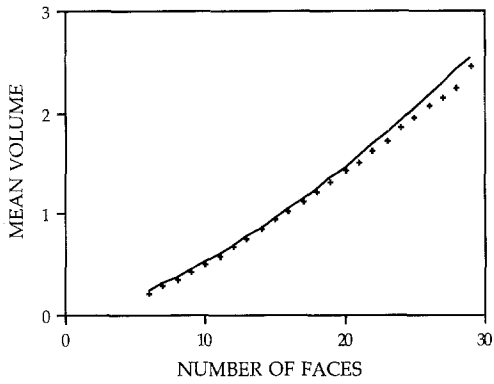

Fig. 7. Mean volume of Voronoi cells having a fixed number of faces. This is based on 102,000 simulated cell data. See Table I and text for the description of the volume normalization factor. (+) The observed data; solid curve shows the best-fit curve $\bar{V}_F = 0.0164F^{1.498}$, where $\bar{V}_F$ is the mean cell volume of an F-faced cell.

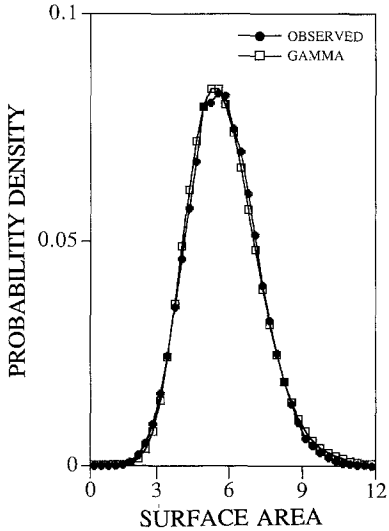

Fig. 8. The probability density distribution of surface area of Voronoi cells in 3D Voronoi tesselation. This is based on 102,000 simulated cell data. The surface area data were grouped in equal intervals of width 0.3040. The best-fit gamma distribution with parameters $a = 15.4847$ and $b = 0.3778$ is also shown. See Table I and text for the description of the surface area normalization factor.

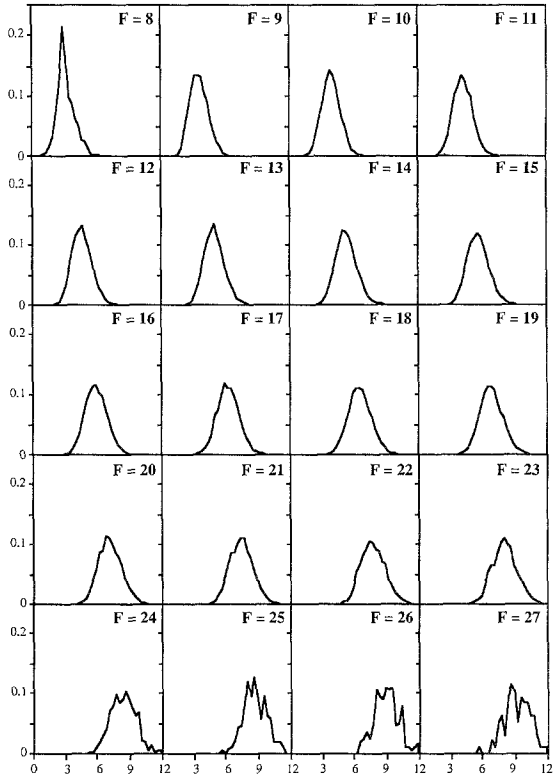

Fig. 9. The probability density distribution of surface area of Voronoi cells having a fixed number of faces F. This is based on 102,000 simulated cell data. The surface area data were grouped in equal intervals of width 0.3040. See Table I and text for the description of the surface area normalization factor. The vertical axis and the horizontal axis denote the probability density and the surface area, respectively. All the curves can be described by the gamma distribution with suitable parameters (listed in Table VII).

$b = 0.282$. These values of a and b give max $|f_{\text{obs}} - f_{\text{fit}}|$ of 0.00256,[7] which is about 2.5 times higher than the 1% Kolmogrov–Smirnov limit 0.00107 (as the sample size used, $n = 2 \times 10^6$, was very large, this difference is not significant). Note also that the mean value ab works out to be 5.994, which is within 0.1% of the theoretical value $\bar{n} = 6$.

In three dimensions, the discretized gamma distribution is a good approximation to the distribution of Voronoi cell faces. The best-fit gamma distribution has $a = 21.6296$ and $b = 0.7199$ ($ab \cong 15.57$); for these values of

[7] max $|f_{\text{obs}} - f_{\text{fit}}|$ is the maximum of the absolute difference between the fitted and the observed cumulative distribution functions.

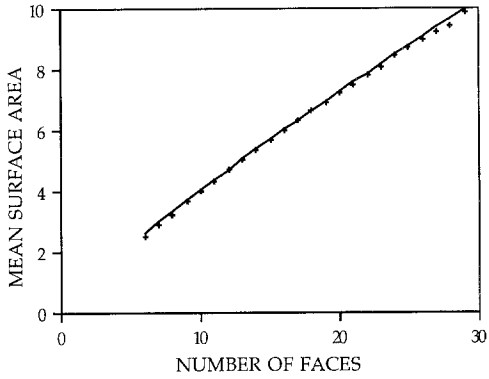

Fig. 10. Mean surface area of Voronoi cells having a fixed number of faces. This is based on 102,000 simulated cell data. See Table I and text for the description of the surface area normalization factor. (+) The observed data; the solid curve shows the best-fit curve $\bar{S}_F = 0.5614F^{0.8526}$, where $\bar{S}_F$ is the mean surface area of an F-faced cell.

a and b, $\max |f_{obs} - f_{fit}|$ is 0.00372, which is slightly higher than the 1% Kolmogrov–Smirnov limit 0.00254 (for $n = 358{,}000$).

Our study also shows that for the face distribution in three dimensions, the discretized lognormal distribution with parameters $\sigma_{ln} = 0.2131$ and $x_{50} = 2.7226$ satisfies the 1% and 5% Kolmogrov–Smirnov limits up to 13,000 and 8,000 Voronoi cell data, respectively. The values of 1% and 5% Kolmogrov–Smirnov limits are $1.52/\sqrt{n}$ and $1.22/\sqrt{n}$, respectively.

One remarkable point of similarity in the two- and three-dimensional Voronoi tesselations is that the coefficient of variation ($= 1/\sqrt{a}$ in the case

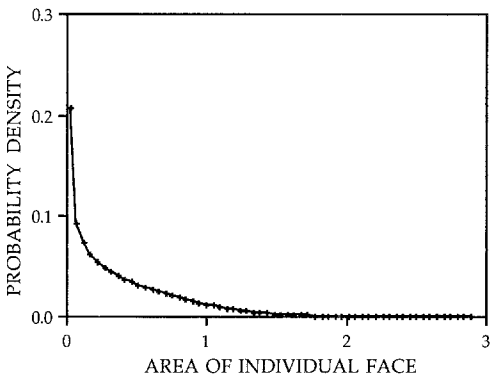

Fig. 11. The probability density distribution of area of individual faces for 3D Voronoi tesselation. This is based on 102,000 simulated cell data. The face area data were grouped in equal intervals of width 0.0485. See Table I and text for the description of the face area normalization factor.

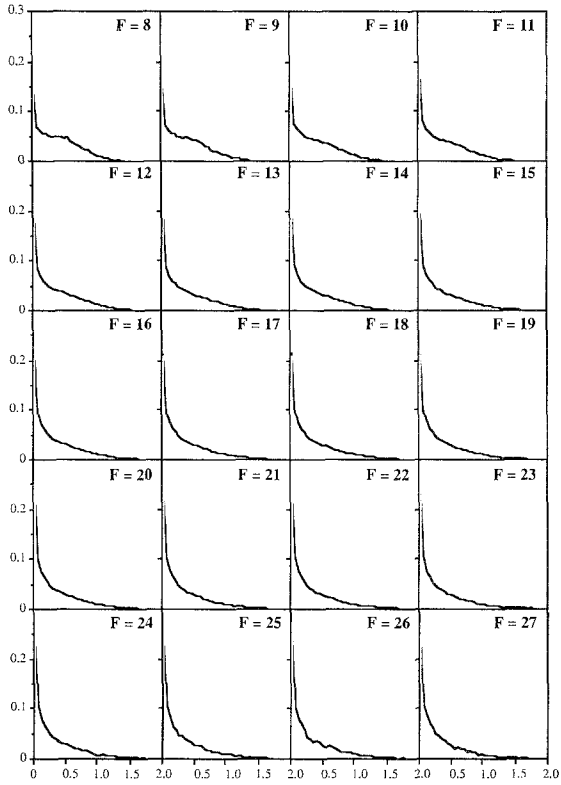

Fig. 12. The probability density distribution of the area of individual faces for Voronoi cells having a fixed number of faces F. This is based on 102,000 simulated cell data. The face area data were grouped in equal intervals of width 0.0485. See Table I and text for the description of the face area normalization factor. The vertical axis and the horizontal axis denote the probability density and the individual face area, respectively.

of the gamma distribution, 0.2169 in two dimensions, and 0.2150 in three dimensions) is substantially independent of dimensionality. It would be intriguing if this result were valid for arbitrary dimensionality.

As each Voronoi cell satisfies the two conditions $V+F-E=2$ and $V=2F-4$, the distributions for the edges and the vertices are not independent. The mean for these two distributions can be calculated from the above two equations:

$$\begin{aligned} \text{mean number of vertices} &= 2\bar{F}-4 \\ &= 27.0862 \\ \text{mean number of edges} &= 3\bar{F}-6 \\ &= 40.6293 \end{aligned}$$

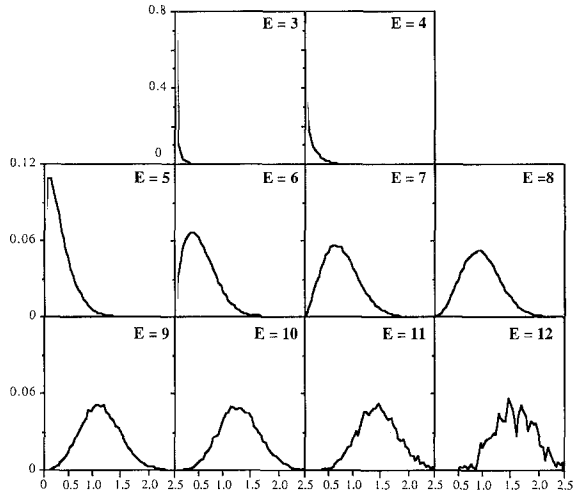

Fig. 13. The probability density distribution of area of individual faces having a fixed number of edges E. This is based on 102,000 simulated cell data. The face area data were grouped in equal intervals of width 0.0485. See Table I and text for the description of the face area normalization factor. The vertical axis and the horizontal axis denote the probability density and the individual face area, respectively.

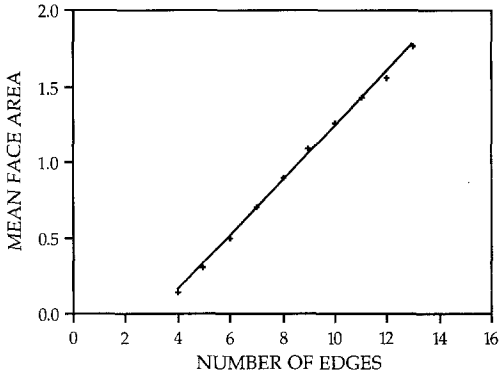

Fig. 14. Mean area of faces having a fixed number of edges. This is based on 102,000 simulated cell data. See Table I and text for the description of the face area normalization factor. (+) The observed data; the straight line shows the best-fit straight line $(\overline{FA})_n = -0.57251 + 0.18124n$, where $(\overline{FA})_n$ is the mean area of an n-sided face, $n = 4, 5, ..., 13$.

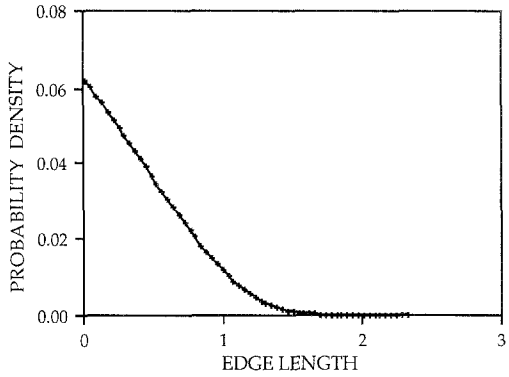

Fig. 15. The probability density distribution of the length of individual edges in 3D Voronoi tesselations. This is based on 102,000 simulated cell data. The edge length data were grouped in equal intervals of width 0.0390. See Table I and text for the description of the edge length normalization factor.

These values are very close to the Meijering's[15] values of 27.0710 and 40.6065, respectively.

The mean number of edges per face, 5.228, is very close to the expected value 5.226,[23] and also to 5.20 ± 0.06, the value given by Mackay[2] for inorganic crystal structures.

We found that the maximum and the minimum numbers of faces in our study were 36 and 4, respectively, whereas those reported earlier were 31[21] and 5,[17] respectively. We also found several 15-edged faces, whereas the earlier reported maximum number of edges in a face was 14.[17]

For F-faced Voronoi cells, the mean number of edges per face $\bar{E}_F$ is equal to $6 - 12/F$. As $F \to \infty$, this value asymptotically approaches to 6, which is equal to the mean number of edges for the two-dimensional Voronoi polygons.

4.2. Volume Distribution

The mean and variance for the cell volume distribution, obtained from 102,000 simulated cells, are very close to the expected values, as shown in Table II.

Kiang[18] suggested $a = 6.0$ and $b = 1/6.0$ as the gamma distribution parameters for the cell volume distribution; whereas Andrade and Fortes[16] suggested $a = 5.56$ and $b = 1/5.56$. Our study shows that if we insist on a mean volume of 1.0, i.e., $ab = 1.0$, then the best-fit gamma distribution parameters are $a = 5.7869$ and $b = 1/a$. However, for these values

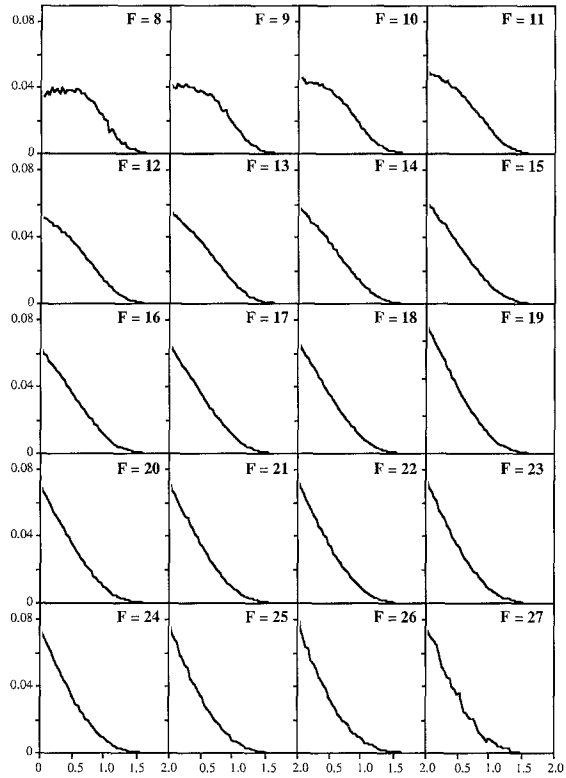

Fig. 16. The probability density distribution of the length of individual edges of Voronoi cells having a fixed number of faces F. This is based on 102,000 simulated cell data. The edge length data were grouped in equal intervals of width 0.0390. See Table I and text for the description of the edge length normalization factor. The vertical axis and the horizontal axis denote the probability density and the individual edge length, respectively.

the maximum of the absolute difference between the observed cumulative probability function and the fitted cumulative probability function, $\max |f_{obs} - f_{fit}|$, is 0.00514, which is slightly higher than the 1% critical Kolmogrov–Smirnov limit $1.52/\sqrt{n}$ ($=0.00476$).

If we look for the best gamma distribution fit irrespective of the value of the mean, then our study shows that $a = 5.6333$ and $b = 0.1782$ ($ab = 1.0004$) gives the best fit and the value of $\max |f_{obs} - f_{fit}|$ in this case is 0.00289, which is below the 5% critical Kolmogorov–Smirnov limit $1.22/\sqrt{n}$ ($=0.00382$).

It is worth mentioning here that in the one-dimensional case, the distribution of the segment lengths obtained by the Voronoi partition of a

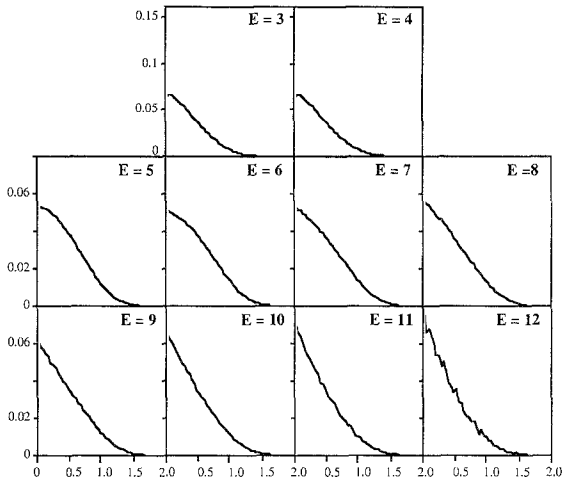

Fig. 17. The probability density distribution of the length of individual edges in faces having a fixed number of edges E. This is based on 102,000 simulated cell data. The edge length data were grouped in equal intervals of width 0.0390. See Table I and text for the description of the edge length normalization factor. The vertical axis and the horizontal axis denote the probability density and the individual edge length, respectively.

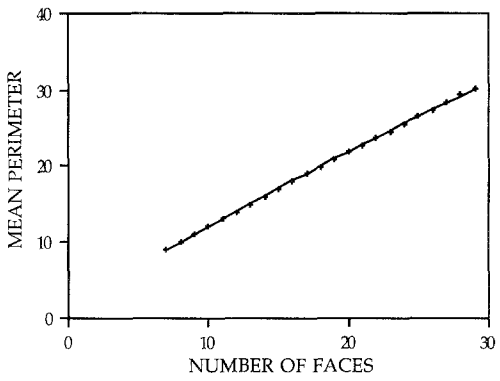

Fig. 18. Mean perimeter of Voronoi cells having a fixed number of faces. This is based on 102,000 simulated cell data. See Table I and text for the description of the edge length normalization factor. (+) The observed data; the solid curve shows the best-fit curve $(\overline{TE})_F = 1.6552F^{0.8596}$, where $(\overline{TE})_F$ is the mean total edge length of an F-faced cell.

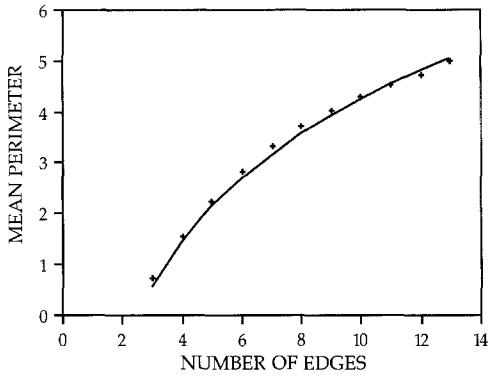

Fig. 19. Mean perimeter of faces having a fixed number of edges. This is based on 102,000 simulated cell data. See Table I and text for the description of the edge length normalization factor. (+) The observed data; the solid curve shows the best-fit curve $(\overline{TE})_n = -2.7968 + 3.0534 \log_e n$, where $(\overline{TE})_n$ is the mean total edge length of an n-sided face.

straight line is a gamma distribution with $a = 2$ and $b = 0.5$,[18] and also, Weaire *et al.*[22] showed by computer simulation that the cell area distribution in a two-dimensional Voronoi partition is best described by the gamma distribution with $a = 3.61$ and $b = 1/a$.

Hanson[17] suggested a Maxwell distribution function defined as

$$P_{x,x+dx} = \frac{32}{\pi^2} e^{-(4/\pi)x^2} dx$$

for the volume distribution of the three-dimensional Poisson–Voronoi cells.

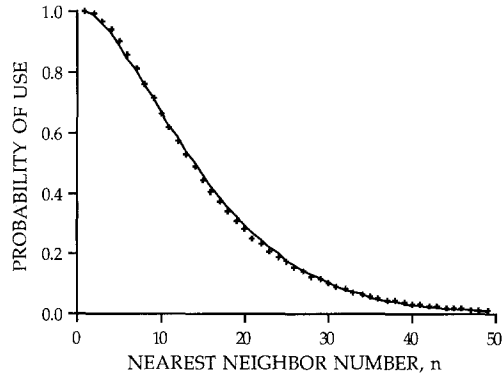

Fig. 20. Probability of the nth-nearest-neighbor Voronoi cell sharing a common face. This is based on data for 148,000 simulated cells. (+) The observed data; the solid curve shows the best-fit curve[17] $P_n = \exp[-0.01471(n-1)^{1.5}]$, where P_n is the probability of the use of the nth neighbor of a point in forming a Voronoi cell face.

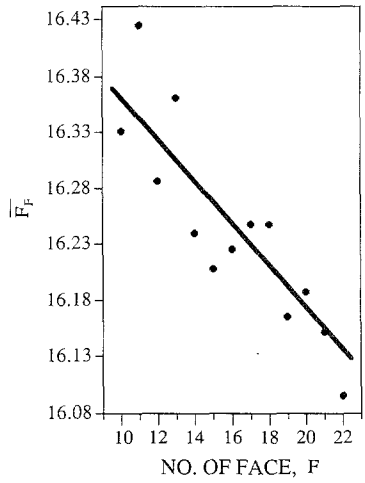

Fig. 21. The joint probability distribution of faces. The vertical axis $\bar{F}_F$ denotes the mean number of faces for the neighboring cells of a cell having F faces. (+) The observed data; the straight line shows the best-fit straight line $\bar{F}_F = 16.57 - 0.02F$.

The relationship becomes

$$n = \frac{32N}{\pi^2}\left(\frac{v}{\bar{v}}\right)^2 e^{-(4/\pi)(v/\bar{v})^2}\frac{dv}{\bar{v}}$$

where n is the expected number of observations in any interval of width $(dv/\bar{v})$ and N is the total number of cases observed. For the Maxwell distribution, the value of $\max|f_{\text{obs}} - f_{\text{fit}}|$ is 0.019137, which is very high relative to the 1% critical Kolmogrov–Smirnov limit of 0.00476. Hence, we conclude that the gamma distribution gives a better fit to the cell volume distribution than the Maxwell distribution.

Kurtz and Carpay[11] suggested the lognormal distribution for the grain volume distribution. Our study shows that for the volume distribution of the Voronoi cell, the lognormal distribution with parameters $\sigma_{\ln} = 0.4332$ and $x_{50} = -0.0735$ satisfies 1% and 5% KS limits up to 7000 and 5000 Voronoi cell data, respectively.

The cell volume distribution for a fixed number of faces F is also found to be best described by the gamma distribution with suitable parameters. The values of the parameters for such classes of faces are listed in Table VI.

Figure 7 shows the plot of mean cell volume for a fixed number of faces $\bar{V}_F$ vs. F. The curve can be described by the equation

$$\bar{V}_F = 0.0164F^{1.498}$$

where $\bar{V}_F$ is the mean cell volume of an F-faced cell, and F is the number of faces, 6–29.

For $F = 15.5355$, i.e., for the mean number of faces, from the above equation, $\bar{V}_F = 0.9987$, which is very close to the expected value for the volume of the three-dimension Poisson–Voronoi cell, i.e., 1.0.

4.3. Surface Area Distribution

The mean surface area of the simulated Voronoi cells is very close to the expected value, as shown in Table II. The cell surface area distribution is best described by a gamma distribution with parameters $a = 15.4847$ and $b = 0.3778$. In this case max $|f_{obs} - f_{fit}|$ is 0.00785, which is about 1.5 times higher than the 1% critical Kolmogrov–Smirnov value $1.52/\sqrt{n}$, i.e., 0.00476 (remembering that the sample size used was very large, $n = 102{,}000$). If we insist on a mean of 5.8209, then the best-fit gamma distribution has the parameters $a = 16.1576$ and $b = 0.3603$, and max $|f_{obs} - f_{fit}|$ is 0.01480.

Our study shows that for the surface area distribution of a Voronoi cell, the lognormal distribution with parameters $\sigma_{ln} = 0.2533$ and $x_{50} = 1.7436$ satisfies 1% and 5% Kolmogrov–Smirnov limits up to 7000 and 4000 Voronoi cell data, respectively. The cell surface area distribution for a fixed number of faces is also best described by the gamma distribution with suitable parameters. The values of the parameters for such classes of faces are listed in Table VII. Figure 10 shows the plot of mean cell surface area for a fixed number of faces $\bar{S}_F$ vs. F. The curve can be described by the equation

$$\bar{S}_F = 0.5614F^{0.8526}$$

where $\bar{S}_F$ is the mean surface area of an F-faced cell, and $F = 6$–29.

For $F = 15.5355$, i.e., for the mean number of faces, from the above equation, $\bar{S}_F = 5.8210$, which is very close to the expected value for the surface area of the three-dimensional Poisson–Voronoi cell, i.e., 5.8209.[15]

4.4. Area of Individual Faces

A plot of the mean area of an n-sided face versus n is shown in Fig. 14. As shown in the figure, the mean area of a face varies linearly as the number of sides n. Using the least square method, one can write a linear relation

$$(\overline{FA})_n = -0.57251 + 0.18124n$$

where $(\overline{FA})_n$ is the mean area of an n-sided face, and $n = 4, 5, \ldots, 13$.

For the three-dimensional Poisson–Voronoi cell, the expected number of edges in a face is equal to 5.226.[23] From the above equation, for $n = 5.226$, the mean area of a face is equal to 0.3747, which is equal to the expected area of a face ($= 5.8209/15.5355$).

4.5. Edge Length Distribution

As shown in Fig. 15, the probability density distribution of the length of individual edges is linear for a considerable length. Thereafter, it drops off at a slower rate. The variation of the mean total edge length of an F-faced Voronoi cell with respect to F is shown in Fig. 18. The equation for the mean total edge length of an F-faced Voronoi cell can be written as

$$(\overline{TE})_F = 1.6552F^{0.8596}$$

where $(\overline{TE})_F$ is the mean total edge length of an F-faced cell, and $F = 7$–31.

For $F = 15.5355$, i.e., for the mean number of faces, from the above equation, the mean total edge length for the Voronoi cell is equal to 17.4950, which is very close to the expected value of 17.4956.[15]

The variation of the mean total edge length, i.e., perimeter, for an n-sided face with respect to n is shown in Fig. 19. The equation for the perimeter of an n-sided face can be approximated by

$$(\overline{TE})_n = -2.7968 + 3.0534 \log_e n$$

where $(\overline{TE})_n$ is the mean total edge length of an n-sided face, and $n = 3$–13.

For the expected number of edges in a face, i.e., $n = 5.226$,[23] from the above equation the mean total edge length per face is equal to 2.2524, which is very near to its expected value of 2.2523 ($= 2 \times 17.4956/15.5355$).

4.6. Nearest Neighbor Use

Hanson[17] suggested the equation

$$P_n = \exp[-0.01471(n-1)^{1.5}]$$

for the probability distribution of the use of the nth neighbor of a point in forming a Voronoi cell face. Figure 20 is based on 148,000 simulated cell data. The function P_n predicts slightly lower probabilities of use for the second to eight nearest neighbors than the observed probabilities, and slightly higher probabilities of use for the 9th to 29th nearest neighbors, and fits the data well beyond the 29th neighbors.

Hanson[17] found two faces at the 98th nearest neighbor, but we found three faces, one each at the 115th, 119th, and 138th nearest neighbors.

4.7. Correlation of Faces

We generated 10,000 Poisson points within a cube having side lengths equal to 1.30 and, using the algorithm described above, simulated the Voronoi cells within a unit cube (of unit length) in the center of the original cube. We discarded those cells which had some portions on the unit cube faces, to eliminate any boundary effect. Finally, we had the data for 3729 Voronoi cells. The mean number of faces for the neighboring cells of the F-faced Voronoi cell is shown in Fig. 21. By using the least squares method, the results can be written as

$$\bar{F}_F = 16.57 - 0.02F$$

where $\bar{F}_F$ is the mean number of faces for the neighboring cells of an F-faced cell.

5. CONCLUSION

A detailed statistical analysis of the three-dimensional cellular microstructure generated by a Poisson–Voronoi tesselation was carried out for up to 358,000 cells using Monte Carlo methods. The results show that a two-parameter gamma distribution gives an accurate fit to the distribution of faces, volumes, and surface areas of the cells. The cell volume and surface area distributions for a fixed number of faces are also found to be best described by the gamma distribution. Distributions of the areas of individual cell faces and the edge lengths were also obtained, but no well-known distribution was found to accurately describe them. For cellular microstructures limited to several thousand cells or less, a two-parameter lognormal distribution was found to give an accurate fit at a 5% level of significance for the distributions of cell faces, surface areas, and volumes.

ACKNOWLEDGMENTS

Financial support for this work was provided by Murata Corporation. Computations were performed on the IBM 3090 at the Center for Academic Computing, Pennsylvania State University, whose assistance is gratefully acknowledged. We also acknowledge helpful discussions of this work with Nandini Kannan, Department of Statistics, Pennsylvania State University.

REFERENCES

1. A. J. Rahman, *J. Chem. Phys.* **45**:2585 (1966).
2. A. L. Mackay, *J. Microsc.* **95**(2):217–227 (1972).

3. F. M. Richards, *Annu. Rev. Biophys. Bioeng.* **6**:151–176 (1977).
4. V. Icke and R. Van de Weygaert, *Astron. Astrophys.* **1987**:16–32.
5. R. Van de Weygaert and V. Icke, *Astron. Astrophys.* **213**:1–9 (1989).
6. D. Weaire and J. P. Kermode, *Phil. Mag. B* **50**:379 (1984).
7. J. L. Finney, *J. Mol. Biol.* **96**:721 (1975).
8. A. Getis and B. Boots, *Models of Spatial Processes* (Cambridge University Press, Cambridge, 1979).
9. C. S. Smith, *Metal Interfaces* (American Society for Metals, Cleveland, Ohio, 1952).
10. F. N. Rhines and K. R. Craig, *Metall. Trans.* **5A**:413 (1974).
11. S. K. Kurtz and F. M. A. Carpay, *J. Appl. Phys.* **51**:5725 (1980).
12. H. V. Atkinson, *Acta Metall.* **36**:469–491 (1988).
13. A. L. Hinde and R. E. Miles, *J. Stat. Comput. Simul.* **10**:205–223 (1980).
14. E. N. Gilbert, *Ann. Math. Stat.* **33**:958 (1962).
15. J. L. Meijering, *Philips Res. Rep.* **8**:270–290 (1953).
16. P. N. Andrade and M. A. Fortes, *Phil. Mag. B* **58**:671–674 (1988).
17. H. G. Hanson, *J. Stat. Phys.* **30**:591 (1983).
18. T. Kiang, *Z. Astrophys.* **64**:433–439 (1966).
19. K. W. Mahin, K. Hanson, and J. W. Morris, Jr., *Acta Metall.* **28**:443–453 (1980).
20. M. F. Vaz and M. A. Fortes, *Scripta Metall.* **22**:35–40 (1988).
21. M. P. Quine and D. F. Watson, *J. Appl. Prob.* **21**:548–557 (1984).
22. D. Weaire, J. P. Kermode, and J. Wejchert, *Phil. Mag. B* **53**:L101–105 (1986).
23. L. A. Santalo, *Integral Geometry and Geometric Probability* (Addison-Wesley, Reading, Massachusetts, 1976).